JOURNAL OF VISUAL COMMUNICATION AND IMAGE REPRESENTATION
Vol. 1, No. 1, September, pp. 104–111, 1990

The Retinal Rod as a Chemical Photomultiplier

MALVIN C. TEICH AND TAO LI

Department of Electrical Engineering, Columbia University, New York, New York 10027

Received December 4, 1989

In vertebrates, the excitation of the retinal rod photoreceptors by a single photon can be represented by a cyclic-GMP cascade. We construct a mathematical model for describing this mechanism and conduct a noise analysis of the process. Our results show that the relative noise of the rod photocurrent, which ensues from a filtering of the discrete multiplication process, is determined primarily by the first stage of the excitatory cascade. This stage is associated with the activation of transducin in the rod outer segment. Our analysis also shows that the conversion of the discrete multiplied signal into a current reduces the output relative noise when it is measured in terms of the variance-to-mean ratio. © 1990 Academic Press, Inc.

1. INTRODUCTION

Visual transduction begins with the conversion of photons into neural electrical signals that are transmitted to higher centers in the nervous system. Experiments have shown that the vertebrate's retinal rod can respond to the absorption of even a single photon [1–7]. In response to an input photon, the toad's rod outer segment (ROS) generates a sodium ion current impulse with an amplitude of 1 ± 0.2 pA and a duration of about 1 s [3]. This means that a single photon blocks about 6 million sodium ions from flowing across the ROS plasma membrane. The rod therefore functions as an amplifier with a particle mean multiplication (gain) of about 6×10^6. However, like all other amplifiers, the rod is not perfect; it generates noise while converting optical information into electrical information [3, 8]. It is of interest to explore the nature of this amplification noise.

A great deal of work has been carried out concerning the behavior of the ROS. As seen in Fig. 1a, a photon absorbed by one of the disk membranes in the ROS first activates a rhodopsin (denoted by R^*) [9] which then acts as an enzyme in the excitation of about 500 transducins (denoted by T) [10–13]. (This number is from *in vitro* studies and probably represents an upper limit.) Each of these excited transducins, in turn, triggers a phosphodiesterase (PDE), an enzyme specific to the molecule cyclic guanosine monophosphate (cGMP) [14, 6]. The activated phosphodiesterase (PDE*) cleaves about 800 cGMP/s [15, 16], thereby decreasing the concentration of cGMP in the ROS which closes the sodium ion channels in the plasma membrane [17, 18, 6]. It has been shown that each activated rhodopsin causes the closing of about 240 sodium channels in the ROS plasma membrane [6], and each of these closed channels blocks the influx of about 2.6×10^4 sodium ions per second [19, 20]. On the basis of this sequence of events we construct a cascade model of the process and use it to analyze the rod signal elicited by a single photon in Section 2. The extension to a Poisson stream of photons impinging on the rod is discussed in Section 3. The discussion is provided in Section 4, and the conclusions are presented in Section 5.

2. ROD OUTER SEGMENT RESPONSE TO SINGLE PHOTONS

A. *Ionic Count Mean and Variance*

A discrete branching process is a random point process in which an initial event (particle) produces a random number of daughter particles at the first stage; each of these daughter particles independently produces a random number of granddaughter particles at the second stage, and so on. The photomultiplier tube (PMT), one of the oldest and most versatile light detectors, is described by this kind of branching process [21, 22]. If we define m as the random variable representing the total number of events at the output of the device for a single input event, then for a device with n stages [21, 22],

$$\overline{m} = \prod_{k=1}^{n} \delta_k \tag{1}$$

$$\sigma_m^2 = \overline{m}^2 \left(\frac{\sigma_1^2}{\delta_1^2} + \frac{\sigma_2^2}{\delta_1 \delta_2^2} + \cdots + \frac{\sigma_n^2}{\delta_1 \delta_2 \cdots \delta_n^2} \right) \tag{2}$$

$$\frac{\sigma_m}{\overline{m}} = \left(\frac{\sigma_1^2}{\delta_1^2} + \frac{\sigma_2^2}{\delta_1 \delta_2^2} + \cdots + \frac{\sigma_n^2}{\delta_1 \delta_2 \cdots \delta_n^2} \right)^{1/2}, \tag{3}$$

where $\overline{m}$ and σ_m^2 are the mean and the variance of the output particle number m, respectively, whereas δ_k and σ_k^2 are the mean and the variance of the random gain at

1047-3203/90 $3.00

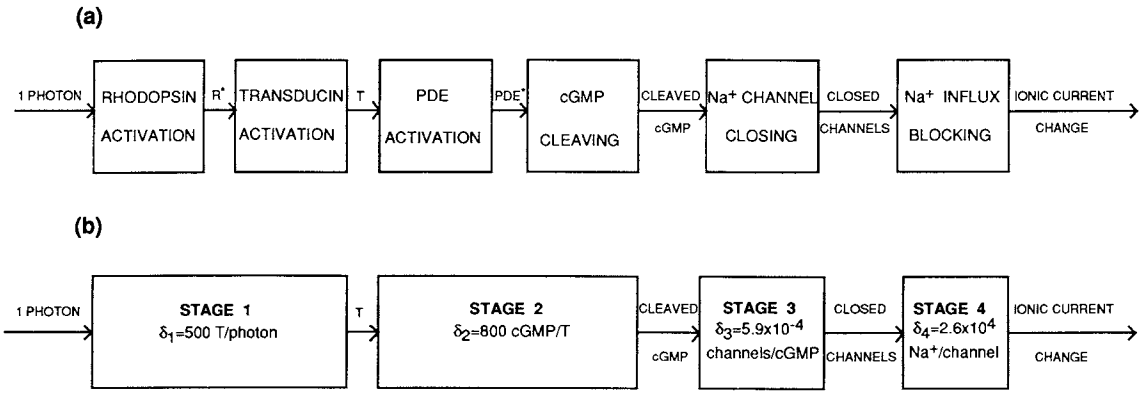

FIG. 1. (a) Physiological representation of photon-induced hyperpolarization of the rod outer segment. (b) A four-stage cascade model for analyzing phototransduction in the rod. The mean multiplication (gain) δ is shown for each stage, in accordance with the well-established experimental values.

the kth stage, respectively. Equation (3) represents the coefficient of variation (CV) for m, which is one measure of the relative noisiness of m.

As described in the previous section, the rod excitatory process consists of six sequential photobiochemical steps (Fig. 1a). Since the first step (excitation of rhodopsin by a photon) is a one-to-one reaction, which means that one photon excites only one rhodopsin, and so is the third step (excitation of PDE by transducin), there are only four stages of amplification involved in the rod excitatory process. Therefore, we might model the process as a four-stage cascade with a mean gain δ of each stage given approximately by 500, 800, 5.9×10^{-4}, and 2.6×10^4, respectively (Fig. 1b). Comparing this model with the photon–electron cascade in the PMT [21], we can see that the rod works like a four-stage chemical photomultiplier, in which the "particles" are transducins, cleaved cGMP molecules, closed Na^+ ion channels, and blocked Na^+ ion numbers, respectively.

Defining the total number of sodium ions blocked due to one photon being absorbed as the random variable m, then according to (1) and (2),

$$\overline{m} = \delta_1\delta_2\delta_3\delta_4] \tag{4}$$

$$\sigma_m^2 = \overline{m}^2\left(\frac{\sigma_1^2}{\delta_1^2} + \frac{\sigma_2^2}{\delta_1\delta_2^2} + \frac{\sigma_3^2}{\delta_1\delta_2\delta_3^2} + \frac{\sigma_4^2}{\delta_1\delta_2\delta_3\delta_4^2}\right) \tag{5}$$

$$\frac{\sigma_m}{\overline{m}} = \left(\frac{\sigma_1^2}{\delta_1^2} + \frac{\sigma_2^2}{\delta_1\delta_2^2} + \frac{\sigma_3^2}{\delta_1\delta_2\delta_3^2} + \frac{\sigma_4^2}{\delta_1\delta_2\delta_3\delta_4^2}\right)^{1/2}. \tag{6}$$

Equations (4) and (5) provide the mean and the variance of the number of Na^+ ions blocked by a single photon at the rod outer segment. Equation (6) provides the coefficient of variation for this random variable.

B. *Two Measures of Relative Noise*

Two measures commonly used for describing the relative noisiness of a signal are the noise-to-signal ratio NSR and the Fano factor F. The NSR (which is the inverse of the signal-to-noise ratio or SNR) is the square of the coefficient of variation, i.e.,

$$\mathrm{NSR}_m \equiv \left(\frac{\sigma_m}{\overline{m}}\right)^2. \tag{7}$$

The Fano factor is the variance-to-mean ratio, so that

$$F_m \equiv \frac{\sigma_m^2}{\overline{m}} = \overline{m}\left(\frac{\sigma_m}{\overline{m}}\right)^2. \tag{8}$$

It is apparent from the sequence of denominators in (3) that the gain of the first stage δ_1 has a dominant influence on $\sigma_m/\overline{m}$ and consequently on the relative noise through (7) and (8); the higher this gain, the lower the contribution to the relative noise from the subsequent stages. It is this mathematical property that spurred the development of high-gain GaP-first-dynode PMTs [23].

It is natural to inquire whether the rod might somehow use this high first-stage gain property. The question arises as to how high this gain should be in order to practically eliminate the contribution of noise from the subsequent stages to the final output.

To explore this question, we consider several plausible scenarios for the statistics of the particle multiplication. We begin by considering all stages following the first to be noiseless, so that

$$\sigma_2 = \sigma_3 = \sigma_4 = 0. \tag{9}$$

Then from (6) we have

$$\frac{\sigma_m}{\overline{m}} = \frac{\sigma_1}{\delta_1}. \tag{10}$$

Equation (10) represents a lower bound for the CV at the output, since the contributions from the subsequent stages are nonnegative, i.e.,

$$\frac{\sigma_m}{\overline{m}} \geq \frac{\sigma_1}{\delta_1}. \tag{11}$$

Considering next all stages following the first to introduce Poisson multiplication provides

$$\sigma_k^2 = \delta_k, \quad k = 2, 3, 4, \tag{12}$$

since the variance is always identically equal to the mean for the Poisson distribution [24]. In this case (6) leads to

$$\frac{\sigma_m}{\overline{m}} = \left(\frac{\sigma_1^2}{\delta_1^2} + \frac{1}{\delta_1\delta_2} + \frac{1}{\delta_1\delta_2\delta_3} + \frac{1}{\delta_1\delta_2\delta_3\delta_4}\right)^{1/2}. \tag{13}$$

Under the condition

$$\frac{1}{\delta_1\delta_2} + \frac{1}{\delta_1\delta_2\delta_3} + \frac{1}{\delta_1\delta_2\delta_3\delta_4} \ll \frac{\sigma_1^2}{\delta_1^2}, \tag{14}$$

it is clear that

$$\frac{\sigma_m}{\overline{m}} \approx \frac{\sigma_1}{\delta_1}, \tag{15}$$

which is the result obtained in (10).

Finally, considering an even more noisy case in which all of the stages following the first introduce Bose–Einstein (geometric) multiplication provides [24]

$$\sigma_k^2 = \delta_k + \delta_k^2, \quad k = 2, 3, 4, \tag{16}$$

so that, in accordance with (6),

$$\frac{\sigma_m}{\overline{m}} = \left(\frac{\sigma_1^2}{\delta_1^2} + \frac{1}{\delta_1} + \frac{2}{\delta_1\delta_2} + \frac{2}{\delta_1\delta_2\delta_3} + \frac{1}{\delta_1\delta_2\delta_3\delta_4}\right)^{1/2}. \tag{17}$$

If

$$\frac{1}{\delta_1} + \frac{2}{\delta_1\delta_2} + \frac{2}{\delta_1\delta_2\delta_3} + \frac{1}{\delta_1\delta_2\delta_3\delta_4} \ll \frac{\sigma_1^2}{\delta_1^2} \tag{18}$$

then we again have

$$\frac{\sigma_m}{\overline{m}} \approx \frac{\sigma_1}{\delta_1}. \tag{19}$$

Thus, if (14) and (18) are obeyed (as will be shown to be true in Appendix B), we find that

$$\frac{\sigma_m}{\overline{m}} \approx \frac{\sigma_1}{\delta_1}, \tag{20}$$

as obtained in (10), (15), and (19) for widely differing multiplication statistics. We conclude that for a single incident photon and any reasonable choice of multiplication statistics, the coefficient of variation of the rod output ion number $\sigma_m/\overline{m}$ is due almost entirely to that of the first stage so that contributions from the subsequent stages can be ignored. Applying (20) to (7) and (8) leads to

$$\mathrm{NSR}_m \approx \left(\frac{\sigma_1}{\delta_1}\right)^2 = \mathrm{NSR}_1, \tag{21}$$

$$F_m \approx \overline{m}\left(\frac{\sigma_1}{\delta_1}\right)^2 = \frac{\overline{m}}{\delta_1} F_1, \tag{22}$$

where NSR_1 and F_1 represent the noise-to-signal ratio and Fano factor at the first stage, respectively. Equations (21) and (22) permit us to conclude that, using both measures, the relative noise of the rod output ionic count triggered by a single photon is principally determined by the relative noise of the first stage of multiplication (transducins per photon).

C. *Ionic Current Pulse Mean and Variance*

The rod photoreceptor converts input photons into output sodium ions in the manner described above. The Na^+ ions are not blocked instantaneously, however. Rather, each photon ultimately results in the switching on of a photocurrent pulse $i(t)$ of duration τ in the ROS (which suppresses the dark current). The result is a current pulse with relatively stable shape and duration, but fluctuating peak amplitude i_0 [3–6]. The statistics of this photocurrent pulse can therefore be approximately described by the random variable i_0 which is related to the ion number m by

$$i_0 = \frac{em}{\tau}, \tag{23}$$

where $e = 1.6 \times 10^{-19}$ C is the electronic charge (charge of a single sodium ion), under the assumption that the pulse shape is rectangular (we relax this restriction in Appendix A). The mean $\overline{i_0}$ and the standard deviation σ_{i_0} of peak amplitude of the current pulse are therefore

$$\bar{i}_0 = \frac{e\bar{m}}{\tau} \tag{24}$$

$$\sigma_{i_0} = \frac{e\sigma_m}{\tau}, \tag{25}$$

so that the coefficient of variation of the current is

$$\frac{\sigma_{i_0}}{\bar{i}_0} = \frac{e\sigma_m/\tau}{e\bar{m}/\tau} = \frac{\sigma_m}{\bar{m}}. \tag{26}$$

The current coefficient of variation is identically equal to the ion-number coefficient of variation. With the help of (7) it is clear that

$$\mathrm{NSR}_{i_0} = \mathrm{NSR}_m, \tag{27}$$

so that the current noise-to-signal ratio is evidently the same as the ion-number noise-to-signal ratio. The relationship is valid for arbitrary current pulse shapes, as shown in Appendix A.

The relation between the Fano factors is not as direct. Using (24), (25), and (8), we find

$$F_{i_0} \equiv \frac{\sigma_{i_0}^2}{\bar{i}_0} = \frac{e}{\tau} F_m, \tag{28}$$

so that the current Fano factor is *not* the same as the ion-number Fano factor. Indeed, the longer the current pulse duration τ, the smaller the Fano factor of the photocurrent. This may be understood in terms of low-pass filtering. The inverse of τ represents the filter bandwidth, so that a larger τ means a smaller filter bandwidth, thereby resulting in a smoothing of the noise. When measured by the Fano factor, the conversion from a random number m into a random current i_0 results in quieting the relative noise as the current pulse duration τ increases.

Combining (21) and (22) with (27) and (28), we obtain

$$\mathrm{NSR}_{i_0} \approx \mathrm{NSR}_1 \tag{29}$$

$$F_{i_0} \approx \left(\frac{e\bar{m}}{\delta_1}\right) \frac{F_1}{\tau}, \tag{30}$$

provided that (20) is satisfied (which it is, as shown in Appendix C). In this case, therefore, the noise-to-signal ratio of the rod photocurrent is controlled only by the noise-to-signal ratio of the first stage of the rod cascade, whereas the Fano factor of the rod photocurrent is controlled by both the Fano factor of the first stage of the rod cascade and the current pulse duration τ.

3. ROD OUTER SEGMENT RESPONSE TO POISSON PHOTONS

In Section 2 we showed that by converting the number of Na^+ ions m resulting from a single photon into a current pulse i, the noise (as measured by the Fano factor) could be smoothed. Almost all light sources produce a Poisson number of photons rather than a single photon, however [24]. It now remains to determine the effect of τ on the relative noise of the rod output and, furthermore, on the behavior of the whole visual information detection system, for a Poisson input photon stream at low light levels (in the absence of saturation). To answer this question we consider two special cases. In the first case the Poisson photons are delivered to the rod in flashes short in comparison with the duration of the current pulse triggered by each single photon, whereas in the other case the Poisson photons are delivered to the rod in the form of steady illumination.

A. *Ionic Current Pulse Mean and Variance for Individual Light Flashes*

When the duration of each flash is short in comparison with the duration of the current pulse triggered by each single photon, we can consider the Poisson photons to be arriving at the rod at the same time. Since the rod output current pulse r is the direct sum of the current pulses triggered by single photons in the absence of saturation, it can be represented as the output of a two-stage cascade, the first stage of which is the Poisson number of photons n and the second stage of which is the current i_0 produced by a single photon. Equations (1) and (2) therefore provide

$$\bar{r} = \bar{n}\bar{i}_0 \tag{31}$$

and

$$\sigma_r^2 = \bar{i}_0^2\sigma_n^2 + \bar{n}\sigma_{i_0}^2. \tag{32}$$

Since n is Poisson distributed, $\sigma_n^2 = \bar{n}$, and we have

$$\sigma_r^2 = \bar{n}(\sigma_{i_0}^2 + \bar{i}_0^2), \tag{33}$$

so that

$$F_r \equiv \frac{\sigma_r^2}{\bar{r}} = F_{i_0} + \bar{i}_0 \tag{34}$$

$$\mathrm{NSR}_r \equiv \frac{\sigma_r^2}{\bar{r}^2} = \frac{\mathrm{NSR}_{i_0} + 1}{\bar{n}}. \tag{35}$$

According to (24) and (28), increasing τ will decrease F_{i_0} and $\bar{i}$ and therefore F_r, but according to (27) and (35), changing τ will not change NSR_r at all.

We now examine the effect that τ might have on the behavior of the detection system as a whole. Considering the rod as the first stage of a visual detection cascade, and defining y and x as variables representing the entire system and the stages lying between the rod and the final output, respectively, (1) and (2) provide

$$\bar{y} = \bar{r}\bar{x} \tag{36}$$

$$\sigma_y^2 = \bar{x}^2\sigma_r^2 + \bar{r}\sigma_x^2, \tag{37}$$

and therefore

$$F_y \equiv \frac{\sigma_y^2}{\bar{y}} = \bar{x}F_r + F_x \tag{38}$$

$$\mathrm{NSR}_y \equiv \frac{\sigma_y^2}{\bar{y}^2} = \mathrm{NSR}_r + \frac{\mathrm{NSR}_x}{\bar{r}}. \tag{39}$$

Since F_r decreases with increasing τ, while $\bar{x}$ and F_x are independent of τ, F_y decreases with increasing τ. According to (31) and (24), $\bar{r}$ decreases with increasing τ, and therefore NSR_y increases with increasing τ, even though NSR_r does not change with τ. Therefore, when a Poisson number of photons is delivered to the rod in a short flash, increasing τ decreases the Fano factor but increases the noise-to-signal ratio of the whole visual detection system.

B. *Ionic Current Mean and Variance for Steady Illumination*

In this case the output current of the rod is shot noise, or to be more specific, generalized shot noise, so that [25]

$$\bar{r} = \mu\int_0^\infty i(t)dt = \mu\int_0^\infty i_0 h(t)dt = \mu\bar{i}_0\int_0^\infty h(t)dt \tag{40}$$

$$\sigma_r^2 = \mu\overline{i^2}\int_0^\infty [h(t)]^2 dt, \tag{41}$$

where μ is the mean rate of the Poisson photon point process, $h(t)$ is the normalized filter function (shape of the current pulse triggered by a single photon, with normalized peak amplitude), and i_0 is the peak amplitude of the current pulse. If we assume $h(t)$ to be rectangular, and define its duration as τ, then

$$\bar{r} = \mu\tau\bar{i}_0 \tag{42}$$

$$\sigma_r^2 = \mu\tau\overline{i_0^2} = \mu\tau(\sigma_{i_0}^2 + \bar{i}_0^2), \tag{43}$$

so that

$$F_r = \frac{\sigma_r^2}{\bar{r}} = F_{i_0} + \bar{i}_0 \tag{44}$$

$$\mathrm{NSR}_r = \frac{\sigma_r^2}{\bar{r}^2} = \frac{\mathrm{NSR}_{i_0} + 1}{\mu\tau}. \tag{45}$$

For nonrectangular shapes we can always take $\int_{-\infty}^{\infty}h(t)dt$ as an equivalent duration τ_e and make $\int_{-\infty}^{\infty}[h(t)]^2dt$ equal to the product of a constant and this τ_e, if the two integrals exist, so that these results still hold. It is clear that (44) takes the same form as (34). Hence increasing τ will again decrease F_r and therefore, from (38), will also decrease F_y. However, unlike the result obtained in (35) for brief light flashes, (45) shows that NSR_r decreases with increasing τ. Applying (45), (42), and (24) to (39) provides

$$\mathrm{NSR}_y = \frac{\mathrm{NSR}_{i_0} + 1}{\mu\tau} + \frac{\mathrm{NSR}_x}{\mu e\bar{m}}, \tag{46}$$

indicating that NSR_y decreases with increasing τ. Therefore, when Poisson photons are delivered to the rod as steady illumination, increasing τ decreases both the Fano factor and the noise-to-signal ratio of the entire visual detection system.

We conclude that when Poisson photons arrive at the rod, the Fano factor of the whole visual information detection system, as well as that of the rod itself, is smaller for large τ for both pulsed and steady light; however, the noise-to-signal ratio of the whole visual information detection system is smaller for large τ only in the case of steady illumination. For pulsed illumination, increasing τ increases NSR_y instead of decreasing it.

4. DISCUSSION

The rod excitatory cascade shown in Fig. 1b prompts us to inquire why the third stage has a very small gain of 5.9×10^{-4}, while the other stages have far larger gains. The noise analysis based on branching process theory provides a possible answer. Referring to (6), it is clear that to produce minimal noise at the output, it is preferable to increase the gain of the early stages to the maximum extent. This means, under the condition of the total gain $\bar{m}$ being fixed (to produce a current of magnitude $\approx$1 pA), that the gain of the later stages must decrease correspondingly. However, because the gain of the final stage δ_4 is the number of sodium ions flowing through a single channel in the plasma membrane of the ROS, decreasing δ_4 would entail increasing the number of channels that are closed by one photon. For an output photocurrent $\approx$1 pA, this would mean that the total number of available sodium ion channels in the plasma membrane of the ROS would have to be increased to preserve the dynamic range of the rod response. However, the sodium ion channel density is $\approx 200/(\mu\mathrm{m})^2$, which would be difficult to increase further [6]. Therefore, practically speaking, the optimal way of minimizing the relative noise is to increase δ_1 and δ_2, and to reduce δ_3, rather than δ_4. Another possibility is that in order to generate the required rapid reaction time, the "off" rate constant of cGMP binding to the channel must be reasonably large and therefore, since the "on" rate constant is limited by diffusional factors, the binding of cGMP to the channel cannot be too tight.

Since the experimental results have shown that the

light-induced decreases in cGMP concentration occur very rapidly compared with the changes in membrane current [17], the kinetics of the first three stages will only influence the latency of the membrane current response and not its time dynamics. This supports the use of a discrete branching process for modeling the phototransduction cascade, in which all of the time dynamics are placed at the final stage where the perturbation in cGMP is converted into a current pulse.

The single-photon rod response can be more thoroughly analyzed by considering random temporal delay and dispersion at each of the four stages. A cascade model of this kind, with Poisson multiplication at each stage, has been developed [26, 27]. In that case, the response $i(t)$ assumes the form of a random function rather than a deterministic function with random peak amplitude i_0. An even more sophisticated treatment of the problem would incorporate the restoration of the cGMP and the reopening of the Na^+ ion channels. However, the experimental measurements indicate a remarkably stable waveform shape and duration, with a peak amplitude i_0 that varies far more than does the normalized current function. It is therefore justified, as a first approximation, to simplify the problem as we have.

5. CONCLUSION

A statistical treatment of the relative noise at the output of the rod has shown that it is governed almost entirely by the noisiness of the first stage of the cascade, even though other stages contribute to the overall gain. Our analysis has shown that the conversion of discrete photons by the rod into the form of a current has the effect of improving the variance-to-mean ratio (Fano factor) of the output signal. As an information detector, the rod photoreceptor exhibits two important characteristics: first, by employing a cascade mechanism, it attains high gain with low noise; second, by converting the signal into the form of a current, it permits the Fano factor to be reduced. Therefore, it may well be that the visual information detection system extracts the Fano factor, although it is usually assumed that the noise-to-signal ratio is the parameter of interest [28].

Finally, it is of interest to compare the performance of the retinal rod with a PMT. The gains of both are similar, $\overline{m} \approx 10^6$–$10^7$ [22]. On the other hand, the noise-to-signal ratio (which is referred to as the modifed excess noise factor in the detection literature [22]) $\mathrm{NSR}_m \approx 0.04$ for the rod, whereas $\mathrm{NSR}_m \approx 0.01$ for a state-of-the-art PMT [22]. In contrast, a near-ideal single-carrier-multiplication conventional avalanche photodiode (APD) has substantially inferior performance: $\overline{m} \approx 10^3$ and $\mathrm{NSR}_m > 1$ [22]. Nevertheless, APDs are widely used because of their small size, low voltage requirements, and durability. The vertebrate rod appears to have most of the advantages of both the PMT and the APD, and few of the disadvantages of either.

APPENDIX A

Validity of Eq. (26) for Arbitrary Current Pulse Shapes

The relationship between an arbitrary current pulse $i(t)$ and the number of electrons in that pulse can be generally described as

$$m = \frac{1}{e}\int_0^\infty i(t)dt = \frac{1}{e}\int_0^\infty i_0 h(t)dt = i_0\left(\frac{1}{e}\int_0^\infty h(t)dt\right), \tag{A1}$$

where i_0 and m are the random variables representing the peak amplitude of the arbitrary current pulse and the number of ions within that pulse, respectively. The function $h(t)$ represents the shape of the arbitrary current pulse (e.g., the shape used by Baylor *et al.* [29]) normalized to unit peak amplitude. We therefore obtain

$$\overline{m} = \frac{\overline{i_0}}{e}\int_0^\infty h(t)dt \tag{A2}$$

$$\sigma_m = \frac{\sigma_{i_0}}{e}\int_0^\infty h(t)dt. \tag{A3}$$

For most pulse shapes $h(t)$, the integral in (A2) and (A3) exists so that an equivalent pulse duration τ_e given by

$$\tau_e = \int_0^\infty h(t)dt \tag{A4}$$

can be defined. Combining this with (A2) and (A3) yields

$$\overline{m} = \frac{\overline{i_0}\tau_e}{e} \tag{A5}$$

and

$$\sigma_m = \frac{\sigma_{i_0}\tau_e}{e}, \tag{A6}$$

respectively, so that

$$\frac{\sigma_{i_0}}{\overline{i_0}} = \frac{\sigma_m}{\overline{m}}, \tag{A7}$$

thereby confirming (26).

APPENDIX B

Validity of Eqs. (14) and (18)

We now verify the validity of (14) and (18), demonstrating that essentially all of the noisiness of the rod

transduction process is associated with photon-to-transducin activation. Using the results of Fung and Stryer [10], Yee and Liebman [15], Stryer [6], and Gray and Attwell [19], we use the approximate values $\delta_1 \approx 500$, $\delta_2 \approx 800$, $\delta_3 \approx 5.9 \times 10^{-4}$, and $\delta_4 \approx 2.6 \times 10^4$. Using the results of Baylor *et al.* [3], on the other hand, we obtain $\overline{i_0} \approx 1$ pA and $\sigma_{i_0} \approx 0.2$ pA, so that (26) gives $\sigma_m/\overline{m} = 0.2$.

If the stages following the first were noiseless ($\sigma_2 = \sigma_3 = \sigma_4 = 0$), according to (10) we would obtain $\sigma_1/\delta_1 = 0.2$.

If the stages following the first introduced Poisson multiplication, according to (13) we would obtain $0.2 = (\sigma_1^2/\delta_1^2 + 2.5 \times 10^{-6} + 4.1 \times 10^{-3} + 1.6 \times 10^{-7})^{1/2}$, so that $\sigma_1/\delta_1 = 0.189 \approx 0.2$, verifying that $(2.5 \times 10^{-6} + 4.1 \times 10^{-3} + 1.6 \times 10^{-7})^{1/2} \approx 0.0041 \ll 0.2^2$. Thus the condition given in (14) is satisfied.

If the stages following the first introduced Bose–Einstein multiplication, according to (17) we would obtain $0.2 = (\sigma_1^2/\delta_1^2 + 2 \times 10^{-3} + 5 \times 10^{-6} + 5.4 \times 10^{-3} + 1.6 \times 10^{-7})^{1/2}$, so that $\sigma_1/\delta_1 = 0.17 \approx 0.2$, verifying that $(2 \times 10^{-3} + 5 \times 10^{-6} + 5.4 \times 10^{-3} + 1.6 \times 10^{-7})^{1/2} \approx 0.0074 \ll 0.2^2$. Thus the condition given in (18) is also satisfied.

Comparing these results, we note that whereas the later stages of the rod cascade change from being modeled as noiseless to very noisy Bose–Einstein, the coefficient of variation of the first stage σ_1/δ_1 changes only slightly, from 0.2 to 0.17. This result implies that the lower bound of σ_1/δ_1 is close to $\sigma_m/\overline{m}$. Fung and Stryer's experiments [10] also support this view, as shown in Appendix C.

APPENDIX C

Validity of Eq. (20)

Fung and Stryer's experiments to study the exchange of GTP for GDP binding on transducins triggered by activated rhodopsins showed first that one activated rhodopsin can excite about 500 transducins (which we discussed in Appendix B), and second that at the saturating light level the excitation of transducins reached a maximum of $31.25 \times 10^{-3} \pm 6.25 \times 10^{-3}$ activated transducins per rhodopsin [10, 6].

Since each rhodopsin is activated by a photon, and the incoming photons follow a Poisson distribution [10], then under the condition of statistical independence for each stage, we can model the transducin excitatory process as a two-stage cascade with the first stage as a Poisson generator. If we define T as the number of activated transducins, T' as the T/rhodopsin, R as the number of rhodopsins, R^* as the number of activated rhodopsins, x_1 as the T/activated rhodopsin, and δ_1 as the mean of x_1, respectively, then according to (1) and (2)

$$\overline{T} = \overline{R^*}\delta_1 \tag{C1}$$

$$\sigma_T^2 = \delta_1^2\sigma_{R^*}^2 + \overline{R^*}\sigma_1^2. \tag{C2}$$

Because R^* is Poisson distributed

$$\overline{R^*} = \sigma_{R^*}^2, \tag{C3}$$

and by (C2) we obtain

$$\sigma_T^2 = \overline{R^*}(\delta_1^2 + \sigma_1^2). \tag{C4}$$

Combining this with (C1) we obtain

$$\frac{\sigma_T}{\overline{T}} = \left(\frac{1}{\overline{R^*}}\left(1 + \frac{\sigma_1^2}{\delta_1^2}\right)\right)^{1/2}. \tag{C5}$$

Since

$$T = RT', \tag{C6}$$

we therefore conclude

$$\overline{T} = R\overline{T'} \tag{C7}$$

$$\sigma_T = R\sigma_{T'} \tag{C8}$$

$$\frac{\sigma_{T'}}{\overline{T'}} = \frac{\sigma_T}{\overline{T}} = \left(\frac{1}{\overline{R^*}}\left(1 + \frac{\sigma_1^2}{\delta_1^2}\right)\right)^{1/2}. \tag{C9}$$

According to Fung and Stryer's data at the maximal excitation $\sigma_{T'}/\overline{T'} = 0.2$, so that

$$\left(\frac{1}{\overline{R^*}}\left(1 + \frac{\sigma_1^2}{\delta_1^2}\right)\right)^{1/2} = 0.2.$$

If

$$\overline{R^*} \geq 26, \tag{C10}$$

then the above equation gives

$$\frac{\sigma_1}{\delta_1} \geq 0.2. \tag{C11}$$

Because the light level is saturated, condition (C10) holds, so (C11) is a lower bound for σ_1/δ_1. Combining this with the upper bound for σ_1/δ_1 obtained from (11), we have $0.2 \leq (\sigma_1/\delta_1) \leq 0.2$, which gives $\sigma_m/\overline{m} = 0.2 \approx \sigma_1/\delta_1$, thereby providing experimental verification for (20).

ACKNOWLEDGMENTS

We are grateful to the anonymous reviewers for helpful suggestions. This work was supported by the National Science Foundation.

REFERENCES

1. S. Hecht, S. Shlaer, and M. H. Pirenne, Energy, quanta, and vision, *J. Gen. Physiol.* **25**, 1942, 819–840.
2. R. D. Penn, and W. A. Hagins, Signal transmission along retinal

rods and the origin of the electroretinographic *a*-wave, *Nature (London)* **223,** 1969, 201–205.

3. D. A. Baylor, T. D. Lamb, and K.-W. Yau, Responses of retinal rods to single photons, *J. Physiol.* **288,** 1979, 613–634.
4. L. Stryer, The molecules of visual excitation, *Sci. Amer.* **257,** 1, 1987, 42–50.
5. J. L. Schnapf, and D. A. Baylor, How photoreceptor cells respond to light, *Sci. Amer.* **256,** 4, 1987, 40–47.
6. L. Stryer, Cyclic GMP cascade of vision, *Annual Rev. Neurosci.* **9,** 1986, 87–119.
7. E. A. Schwartz, Phototransduction in vertebrate rods, *Annual Rev. Neurosci.* **8,** 1985, 339–367.
8. D. A. Baylor, G. Matthews, and K.-W. Yau, Two components of electrical dark noise in toad retinal rod outer segments, *J. Physiol.* **309,** 1980, 591–621.
9. B. Honig, T. Ebrey, R. H. Callender, U. Dinur, and M. Ottolenghi, Photoisomerization, energy storage, and charge separation: A model for light energy transduction in visual pigments and bacteriorhodopsin, *Proc. Nat. Acad. Sci. USA* **76,** 1979, 2503–2507.
10. B. K.-K. Fung, and L. Stryer, Photolyzed rhodopsin catalyzes the exchange of GTP for bound GDP in retinal rod outer segments, *Proc. Nat. Acad. Sci. USA* **77,** 1980, 2500–2504.
11. B. K.-K. Fung, J. B. Hurley, and L. Stryer, Flow of information in the light-triggered cyclic nucleotide cascade of vision, *Proc. Nat. Acad. Sci. USA* **78,** 1981, 152–156.
12. H. Kuhn, Light- and GTP-regulated interaction of GTPase and other proteins with bovine photoreceptor membranes, *Nature (London)* **283,** 1980, 587–589.
13. P. A. Liebman, and E. N. Pugh, Jr., Control of rod disk membrane phosphodiesterase and a model for visual transduction, *Curr. Top. Membr. Transp.* **15,** 1981, 157–260.
14. N. Bennett, Light-induced interactions between rhodopsin and the GTP-binding protein. Relation with phosphodiesterase activation, *Eur. J. Biochem.* **123,** 1982, 133–139.
15. R. Yee, and P. A. Liebman, Light-activated phosphodiesterase of the rod outer segment. Kinetics and parameters of activation and deactivation, *J. Biol. Chem.* **253,** 1978, 8902–8909.
16. N. Miki, J. M. Baraban, J. J. Keirns, J. J. Boyce, and M. W. Bitensky, Purification and properties of the light-activated cyclic nucleotide phosphodiesterase of rod outer segments, *J. Biol. Chem.* **250,** 1975, 6320–6327.
17. R. H. Cote, M. S. Biernbaum, G. D. Nicol, and M. D. Bownds, Light-induced decreases in cGMP concentration precede changes in membrane permeability in frog rod photoreceptors, *J. Biol. Chem.* **259,** 1984, 9635–9641.
18. E. E. Fesenko, S. S. Kolesnikov, and A. L. Lyubarsky, Induction by cyclic GMP of cationic conductance in plasma membrane of retinal rod outer segment, *Nature (London)* **313,** 1985, 310–313.
19. P. Gray, and D. Attwell, Kinetics of light-senstive channels in vertebrate photoreceptors, *Proc. R. Soc. London B* **223,** 1985, 379–388.
20. A. L. Zimmerman, and D. A. Baylor, Electrical properties of the light-sensitive conductance of salamander retinal rods, *Biophys. J.* **47,** 1985, 357a.
21. R. W. Engstrom, *RCA Photomultiplier Handbook (PMT-62)*, RCA Electro Optics and Devices, Lancaster, PA, 1980.
22. M. C. Teich, K. Matsuo, and B. E. A. Saleh, Excess noise factors for conventional and superlattice avalanche photodiodes and photomultiplier tubes, *IEEE J. Quant. Electron.* **QE-22,** 1986, 1184–1193.
23. G. A. Morton, and H. M. Smith, Pulse height resolution of high gain first dynode photomultipliers, *Appl. Phys. Lett.* **13,** 1968, 356–357.
24. M. C. Teich, and B. E. A. Saleh, Photon bunching and antibunching, in *Progress in Optics* (E. Wolf, Ed.), Vol. 26, pp. 1–104, North-Holland, Amsterdam, 1988.
25. S. O. Rice, Mathematical analysis of random noise, *Bell Syst. Tech. J.* **23,** 1944, 282–332 (reprinted in *Selected Papers on Noise and Stochastic Processes* (N. Wax, Ed.), Dover, New York, 1954).
26. K. Matsuo, B. E. A. Saleh, and M. C. Teich, Cascaded Poisson processes, *J. Math. Phys.* **23,** 1982, 2353–2364.
27. K. Matsuo, M. C. Teich, and B. E. A. Saleh, Poisson branching point processes, *J. Math. Phys.* **25,** 1984, 2174–2185.
28. T. N. Cornsweet, *Visual Perception*, Academic Press, New York, 1970.
29. D. A. Baylor, T. D. Lamb, and K.-W. Yau, The membrane current of single rod outer segments. *J. Physiol.* **288,** 1979, 589–611.